Similarities in 2- and 6-Line Ferrihydrite Based on Pair Distribution Function Analysis of X-ray Total Scattering

F. M. Michel,*[,†,‡] L. Ehm,[†,‡] G. Liu,[†,§] W. Q. Han,[⊗] S. M. Antao,[†,‡,▽] P. J. Chupas,[||] P. L. Lee,[||] K. Knorr,[⊥] H. Eulert,[⊥] J. Kim,[†,#] C. P. Grey,[†,#] A. J. Celestian,[†,‡,○] J. Gillow,[†,∞] M. A. A. Schoonen,[†,‡] D. R. Strongin,[†,§] and J. B. Parise[†,‡,#]

Center for Environmental Molecular Science (CEMS), Department of Geosciences, and Department of Chemistry, Stony Brook University, Stony Brook, New York 11794, Department of Chemistry, Temple University, Philadelphia, Pennsylvania 19122, Advanced Photon Source, Argonne National Laboratory, Argonne, Illinois 60439, Christian-Albrechts-Universitaet zu Kiel, Institut fuer Geowissenschaften, Kiel, Germany, 24098, and Center for Functional Nanomaterials and Environmental Sciences Department, Brookhaven National Laboratory, Upton, New York 11973

Received October 30, 2006. Revised Manuscript Received December 14, 2006

Iron(III) hydroxides are abundant in near-surface natural environments and play an important role in geochemical processes and the fate of contaminants. The issue of the structure of the common nanophase material ferrihydrite (ferric hydroxide) is controversial and has been debated in the literature for many years without definitive resolution. At least two types of ferrihydrite, the 2-line and 6-line forms, are conventionally recognized. It has been suggested that these forms possess different structures built up by different mixtures of distinct nanophase components. However, traditional crystallographic methods provide depictions of structure that are most sensitive either to short-range order (X-ray absorption) or long-range periodicity (X-ray diffraction or electron diffraction). We used high-energy X-ray total scattering for pair distribution function analysis to observe both the short- and intermediate-range ordering (exceeding ∼15 Å) of synthetic ferrihydrite with three distinct average domain sizes of 2, 3, and 6 nm. We show that there are no significant differences in the underlying structures of these materials and that the differences in the diffraction patterns can be entirely interpreted by variations in the average size of the coherent scattering domains. The average crystallite sizes inferred from the PDF analysis are in good agreement with direct observation by high-resolution transmission electron microscopy.

Introduction

Ferric hydroxides are important mineral components and the subject of much scientific research in environmental and soil sciences because of their ubiquity in soils, groundwater, and aquatic sediments.[1−3] The oxidation and dissolution through weathering of Fe-bearing sulfide minerals associated with ore deposits and mining activities consequently results in the formation of secondary iron oxides, including ferrihydrite. Its large surface area and high reactivity results in a large adsorptive capacity for toxic contaminants such as U, As, Cd, and Pb.[4] Accordingly, ferrihydrite has been important in metallurgical processing and used as an absorbent to remove contaminants from wastewaters.[5] Ferrihydrite has also been observed in meteorites, and its presence on Mars may have important implications for understanding the magnetic properties of that planet's soils.[6,7]

Ferrihydrite, otherwise commonly referred to as amorphous iron hydroxide, protoferrihydrite, and colloidal or hydrous ferric hydroxide, has long been described as poorly crystalline, disordered, and X-ray amorphous.[8−10] Evidence from direct imaging using electron microscopy,[11] atomic force microscopy (AFM), and scanning tunneling microscopy (STM)[12] indicates that ferrihydrite is a nanosized material. The number of broadened maxima in individual powder X-ray diffraction (XRD) patterns obtained with conventional X-ray sources is customarily used to designate the material as "2-line" or "6-line" ferrihydrite. The most widely reported

* Corresponding author. E-mail: fmichel@ic.sunysb.edu.
† Center for Environmental Molecular Science.
‡ Department of Geosciences, Stony Brook University.
§ Temple University.
|| Argonne National Laboratory.
⊥ Christian-Albrechts-Universitaet zu Kiel.
Department of Chemistry, Stony Brook University.
⊗ Center for Functional Nanomaterials, Brookhaven National Laboratory.
∞ Environmental Sciences Department, Brookhaven National Laboratory.
▽ Current address: Advanced Photon Source, Argonne National Laboratory, Argonne, IL 60439.
○ Current address: School of Earth and Environmental Sciences, City University of New York Queens College, Flushing, NY 11367.

(1) Rancourt, D. G.; Fortin, D.; Pichler, T.; Thibault, P. J.; Lamarche, G.; Morris, R. V.; Mercier, P. H. J. *Am. Mineral.* **2001**, *86* (7−8), 834−851.
(2) Schwertmann, U.; Carlson, L.; Murad, E. *Clays Clay Miner.* **1987**, *35* (4), 297−304.
(3) Shaked, Y.; Erel, Y.; Sukenik, A. *Geochim. Cosmochim. Acta* **2004**, *68* (7), 1439−1451.
(4) Jambor, J. L.; Dutrizac, J. E. *Chem. Rev.* **1998**, *98* (7), 2549−2585.
(5) Dyer, J. A.; Trivedi, P.; Sanders, S. J.; Scrivner, N. C.; Sparks, D. L. *J. Colloid Interface Sci.* **2004**, *270* (1), 66−76.
(6) Bishop, J. L.; Pieters, C. M.; Burns, R. G. *Geochim. Cosmochim. Acta* **1993**, *57* (19), 4583−4595.
(7) Morris, R. V.; Golden, D. C.; Bell, J. F.; Lauer, H. V.; Adams, J. B. *Geochim. Cosmochim. Acta* **1993**, *57* (19), 4597−4609.
(8) Ivarson, K. C.; Sojak, M. *Can. J. Soil Sc.* **1978**, *58* (1), 1.
(9) Schwertmann, U.; Fischer, W. R. *Geoderma* **1973**, *10* (3), 237−247.
(10) Towe, K. M.; Bradley, W. F. *J. Colloid Interface Sci.* **1967**, *24* (3), 384.
(11) Janney, D. E.; Cowley, J. M.; Buseck, P. R. *Clays Clay Miner.* **2000**, *48* (1), 111−119.
(12) Liu, G.; Debnath, S.; Paul, K. W.; Han, W.; Hausner, D. B.; Hosein, H. A.; Michel, F. M.; Parise, J. B.; Sparks, D. L.; Strongin, D. R. *Langmuir* **2006**, *22*, 9313−9321.

10.1021/cm062585n CCC: $37.00
Published on Web 02/03/2007

nominal formula for ferrihydrite is $5Fe_2O_3 \cdot 9H_2O$,[13] although a number of other similar formulas (e.g., $Fe_5HO_8 \cdot 4H_2O$, $Fe(OH)_3$, $Fe_2O_3 \cdot 2FeOOH \cdot 26H_2O$) have also been proposed.[10,14,15]

Despite the numerous studies of this material using a variety of techniques, the structure of ferrihydrite has not yet been solved.[4] The poorly delineated diffraction features have inhibited the use of traditional techniques of structural analysis, resulting in ongoing debate regarding its atomic structure.[11,16−18] There is presently disagreement on whether 2- and 6-line ferrihydrite is best described by a single (defective) phase or by mixtures of phases. Moreover, no consensus has been reached on whether these two materials differ only in domain size or if they also exhibit distinct structural differences. Contemporary models are determined on the basis of a variety of studies conducted using extended X-ray absorption fine structure (EXAFS), wide-angle and anomalous X-ray scattering, neutron diffraction,[17] and electron nanodiffraction.[16,19] Two recent electron diffraction studies by Janney et al. have proposed different multiphase structures models for 2- and 6-line ferrihydrite.[16,19] However, several studies[20−22] support the notion that the primary difference between the least and most crystalline forms of ferrihydrite (i.e., 2- and 6-line, respectively) is the size of the coherent scattering domains. In one such study, Guyodo et al.[21] concluded, using EXAFS analysis of samples with average particle sizes ranging from 3 to 5.4 nm, that the local environment of Fe in these samples is identical. Here, we present results from synchrotron-based X-ray total scattering experiments, which indicate that both the short- and intermediate-range ordering in nanocrystalline ferrihydrite are essentially the same and independent of changes in particle size. We believe that our results represent an important step in quantifying the terms of the so-called 2- and 6-line forms and significantly advance our understanding of the atomic arrangements in nanocrystalline ferrihydrite; this will lead to a better understanding its structure, reactivity, and other interesting properties.

Experimental Section

Ferrihydrite nanoparticles with three different average domain sizes (2, 3, and 6 nm) were prepared using different nonbiological routes that are briefly described. The samples included in the present study will not be referred to by the nomenclature traditionally used to describe the number of diffraction maxima (e.g., 2-, 3-, 6-line, etc.). The term "ferrihydrite" (or abbreviated "Fhyd") will hereinafter be followed by the estimated average coherent scattering domain size (e.g., Fhyd2, Fhyd3, or Fhyd6) when describing the least and most crystalline forms of ferrihydrite, respectively. To evaluate the potential for sample variation resulting from differences in synthesis conditions, our study also included analysis of three samples of 2 nm ferrihydrite made by independent groups at BNL, Temple, and Stony Brook University, with all using the same general preparation method discussed below.

Fhyd2 and Fhyd6 were synthesized using a method developed by Schwertmann and Cornell.[13] For sample Fhyd2, a 1 M solution of NaOH (Sigma-Aldrich) was added at a rate of 2 mL/min to a 0.2 M solution of $Fe(NO_3)_3 \cdot 9H_2O$ (Sigma-Aldrich) with constant stirring until the pH reached 7.5. The solution was repeatedly washed with deionized water (DI) (18 MΩ cm in resistivity) and centrifuged to remove remaining electrolytes. Here, we use centrifuging and drying naturally in a hood because previous studies show that processing ferrihydrite nanoparticles by freeze-drying leads to the formation of more crystalline 3-line ferrihydrite nanoparticles and goethite.[23] Sample Fhyd3 was synthesized using a method adapted from Anschutz and Penn[24] in which 1.0 L of 0.48 M $NaHCO_3$ (Fischer, ACS grade) was added dropwise at a rate of 4.58 mL/min to a continuously stirred 1.0 L solution of 0.40 M $Fe(NO_3)_3 \cdot 9H_2O$ to form a homogeneous dark brownish suspension. The resulting suspension was placed into 200 mL Nalgene bottles and microwaved until boiling occurred. During heating, the bottles were agitated by shaking every 40 s to achieve homogeneous heating of the suspension. Immediately after heating, the suspension was rapidly cooled in an ice bath to room temperature. The suspension was subsequently dialyzed in DI for 3 days, with the water being changed several times daily. Finally, dry samples were prepared by drying them in air. The 6 nm ferrihydrite nanoparticles were synthesized by dissolving 20 g of $Fe(NO_3)_3 \cdot 9H_2O$ into 2 L of DI at a temperature of 75 °C, with rapid stirring for 10−12 min to form a homogeneous dark reddish suspension. The suspension was rapidly cooled inside an ice bath to room temperature and dialyzed in DI for at least 7 days, with the water being changed several times daily. Finally, the suspension was freeze-dried. All chemicals were used as received and without additional purification.

Characterization of ferrihydrite was carried out in part by the collection of high-energy X-ray total scattering data coupled with pair distribution function analysis (PDF). Finely powdered dry samples were loaded into 1 mm polyimide (Kapton) capillaries. A portion of each powdered sample was also redispersed in DI and subsequently loaded into 3 mm polyimide capillaries for analysis in an aqueous medium. Scattering data were collected at the 11-ID-B[25] (~90.3 keV, $\lambda = 0.1372(2)$ Å) and 1-ID-C[26] (~100.1 keV, $\lambda = 0.1238(6)$ Å) beamlines of the Advanced Photon Source (APS). The diffraction data were collected at ambient temperature on either a MAR345 image plate detector system or an Angio detector, an amorphous Si detector manufactured by General Electric. To obtain properly normalized experimental PDFs, we collected diffraction data on both the samples and blanks over a wide Q-range (maximum of ~30 $Å^{-1}$). The independent measurement of the true background intensity by the collection of a blank allows for the direct subtraction

(13) Schwertmann, U.; Cornell, R. M. *Iron Oxides in the Laboratory: Preparation and Characterization*, 1st ed.; Wiley-VCH: Weinheim, Germany, 2000; pp 89−94.
(14) Chukhrov, F. V.; Zvyagin, B. B.; Gorshkov, A. I.; Yermilova, L. P.; Balashove, V. V. *Int. Geol. Rev.* **1973**, *16*, 1131.
(15) Eggleton, R. A.; Fitzpatrick, R. W. *Clays Clay Miner.* **1988**, *36* (2), 111−124.
(16) Janney, D. E.; Cowley, J. M.; Buseck, P. R. *Am. Mineral.* **2000**, *85* (9), 1180−1187.
(17) Jansen, E.; Kyek, A.; Schafer, W.; Schwertmann, U. *Appl. Phys. A: Mater. Sci. Process.* **2002**, *74*, S1004−S1006.
(18) Manceau, A.; Drits, V. A. *Clay Miner.* **1993**, *28* (2), 165−184.
(19) Janney, D. E.; Cowley, J. M.; Buseck, P. R. *Am. Mineral.* **2001**, *86* (3), 327−335.
(20) Drits, V. A.; Sakharov, B. A.; Salyn, A. L.; Manceau, A. *Clay Miner.* **1993**, *28* (2), 185−207.
(21) Guyodo, Y.; Banerjee, S. K.; Penn, R. L.; Burleson, D.; Berauo, T. S.; Seda, T.; Solheid, P. *Phys. Earth Planet. Inter.* **2006**, *154* (3−4), 222−233.
(22) Kukkadapu, R. K.; Zachara, J. M.; Fredrickson, J. K.; Smith, S. C.; Dohnalkova, A. C.; Russell, C. K. *Am. Mineral.* **2003**, *88* (11−12), 1903−1914.
(23) Greffie, C.; Amouric, M.; Parron, C. *Clay Miner.* **2001**, *36* (3), 381−387.
(24) Anschutz, A. J.; Penn, R. L. *Geochem.Trans.* **2005**, *6* (3), 60−66.
(25) Rutt, U.; Beno, M. A.; Strempfer, J.; Jennings, G.; Kurtz, C.; Montano, P. A. *Nucl. Instr. Methods Phys. Res., Sect. A* **2001**, *467*, 1026−1029.
(26) Shastri, S. D.; Fezzaa, K.; Mashayekhi, A.; Lee, W.-K.; Fernandez, P. B.; Lee, P. L. *J. Synchrotron Radiat.* **2002**, (9), 317−322.

Table 1. Experimental Details[a]

sample ID	beamline	λ (Å)	sample-detector distance (mm)	detector type	maximum Q-range (Å^{-1})
	1-ID-C	0.1238(6)	259.8	*a*-Si	23.0−25.0
Fhyd2, 3, and 6	11-ID-B	0.1370(2)	207.9	*a*-Si	∼29.5
	11-ID-B	0.1372(2)	745.5	Mar345	10.1

[a] The reported Q-range corresponds to the range of data incorporated in the transformation of $S(Q)$ to the resulting PDF. The data collected at 11-ID-B using a larger sample-detector distance were not collected for PDF analysis.

of the parasitic scatter (e.g., capillary, aqueous medium (if present)). Equal exposure times were used for each sample and blank. Two blanks were necessary for properly removing background associated with the container (capillary) and water (for the samples redispersed in aqueous solution only). A CeO_2 standard (NIST diffraction intensity standard set 674a) was used to calibrate the sample-to-detector distance and the tilt of the detector relative to the incident beam. The conversion of data from 2D to 1D was performed using the program Fit2D,[27,28] and a polarization correction was applied during integration of the data. The sample-to-detector distance was increased to improve resolution in the low-Q region for certain data collected at 11-ID-B. Details regarding the experimental setup at each beamline and for each sample are included in Table 1.

The total scattering structure function, $S(Q)$, and PDF ($G(r)$) were obtained using PDFgetX2,[29] where standard corrections were applied as well as those unique to the image-plate geometry.[30] The Fourier transform of the normalized and weighted $S(Q)$, or $Q[S(Q)-1]$, results in the PDF, or $G(r)$, which corresponds to real space interatomic distances. The positions of the first three correlations in each PDF were determined from profile fitting with a linear combination of Gaussian and Lorentzian profiles using the program WinPLOTR.[31] The PDF method differs from traditional techniques of X-ray diffraction (e.g., Rietveld) in that it directly yields information on the local, intermediate, and long-range (if present) structure. The PDF method also provides a useful tool for understanding the average scattering domain size of nanocrystalline materials through an evaluation of PDF attenuation.[32−37] In brief, the exponential decay of the PDF can be attributed to a limited range of structural coherence if within the resolution of the instrument, as usually determined by a crystalline standard (e.g., CeO_2). In the case of highly crystalline samples, the exponential decay is primarily an indication of the resolution of the instrument[37] or instrument envelope. The resolution for these two beamlines was determined previously using CeO_2 and was included in earlier communications.[34,35] The presence of structural disorder (e.g., static disorder and/or strain) at the surface or the interior of a nanocrystalline material can also effect the attenuation of the PDF and thereby result in an underestimate of the average crystallite size through the range of structural coherence. Therefore, the extrapolation of average crystallite size on the basis of the range of structural coherence in the PDF should be considered as being a minimum value. This aspect of the PDF has been reviewed elsewhere[36] and was demonstrated in the case of nanocrystalline ZnS.[38] Therefore, the use of a separate technique, such as direct imaging by electron microscopy, is often necessary to corroborate the size estimates from PDF.

High-resolution transmission electron microscopy (HRTEM) was performed using a 300 kV JEOL-3000FEG microscope equipped with an energy-dispersive X-ray spectrometer at Brookhaven National Laboratory (BNL). Fast Fourier transform (FFT) diffraction patterns were taken from the whole areas of selected images. To prepare the TEM samples, first, we redispersed ferrihydrite as a dry powder into DI water and sonicated it in an ice bath to form a homogeneous suspension and prevent any phase transformation to a more stable phase such as goethite or hematite. Second, a drop of the ferrihydrite suspension was placed onto an amorphous holey-carbon film supported by a standard TEM Cu grid (Ted Pella, Inc.). The excess suspension on the TEM grid was removed by absorbing the fluid with filter paper and the samples were allowed to dry at ambient conditions.

Thermogravimetric analysis (TGA) was performed using a Shimadzu DTG-60H apparatus. Weight loss was determined on <30 mg of each sample loaded in an open Pt pan. Heating was carried out at a rate of 10 K/min from ambient to 1073/1273 K under flowing dry N_2.

Results

The initial identification of synthetic ferrihydrite was performed using the low 2θ region of XRD patterns (Figure 1). The resolution was improved in these patterns by increasing the sample-to-detector distance to ∼50 cm at the 11-ID−B beamline. The patterns included in Figure 1 for Fhyd2 and Fhyd6 illustrate how the number of peaks in individual diffraction patterns is customarily used to designate the material as "2-line" or "6-line" ferrihydrite, respectively. The broadened features corresponding to d-spacing values of 0.26, ∼0.20, and 0.15 nm are indicative of those reported in prior studies of ferrihydrite.[4] Because of peak broadening caused by nanocrystalline particle sizes and resulting in diminished intensity and increased overlap, the features in the pattern for Fhyd2 are less pronounced, and some peaks are nearly unrecognizable compared to those of Fhyd6. However, comparison of the diffraction patterns for all three samples reveals the presence of essentially all the same diffraction maxima.

(27) Hammersley, A. P. *Fit2D V9.129 Reference Manual V. 3.1*; ESRF Internal Report, ESRF98HA01T; European Synchrotron Radiation Facility: Grenoble, France, 1998.
(28) Hammersley, A. P.; Svenson, S. O.; Hanfland, M.; Hauserman, D. *High Pressure Res.* **1996**, *14*, 235−248.
(29) Qiu, X.; Thompson, J. W.; Billinge, S. J. L. *J. Appl. Crystallogr.* **2004**, *37*, 110−116.
(30) Chupas, P. J.; Qui, X.; Hanson, J. C.; Lee, P. L.; Grey, C. P.; Billinge, S. J. L. *J. Appl. Crystallogr.* **2003**, *36*, 1342−1347.
(31) Roisnel, T.; Rodriguez-Carvajal, J. WinPLOTR: A Windows Tool for Powder Diffraction Powder Analysis. In *Proceedings of the Seventh European Powder Diffraction Conference* (EPDIC 7), Barcelona, Spain, May 20−23, 2000; Delhez, R., Mittenmeijer, E. J., Eds.; *Mater. Sci. Forum* **2000**, 118−123.
(32) Billinge, S. J. L.; Petkov, V.; Proffen, T. *Commission on Powder Diffraction of the International Union of Crystallography Newsletter* **2000**, 21−22.
(33) Hall, B. D.; Zanchet, D.; Ugarte, D. *J. Appl. Crystallogr.* **2000**, *33*, 1335−1341.
(34) Michel, F. M.; Antao, S. M.; Chupas, P. J.; Lee, P. L.; Parise, J. B.; Schoonen, M. A. A. *Chem. Mater.* **2005**, *17* (25), 6246−6255.
(35) Michel, F. M.; Schoonen, M. A. A.; Zhang, X. V.; Martin, S. T.; Parise, J. B. *Chem. Mater.* **2006**, *18* (7), 1726−1736.
(36) Neder, R. B.; Korsunskiy, V. I. *J. Phys.: Condens. Matter* **2005**, *17* (5), S125−S134.
(37) Page, K.; Proffen, T.; Terrones, H.; Terrones, M.; Lee, L.; Yang, Y.; Stemmer, S.; Seshadri, R.; Cheetham, A. K. *Chem. Phys. Lett.* **2004**, *393*, 385−388.
(38) Gilbert, B.; Huang, F.; Zhang, H. Z.; Waychunas, G. A.; Banfield, J. F. *Science* **2004**, *305* (5684), 651−654.

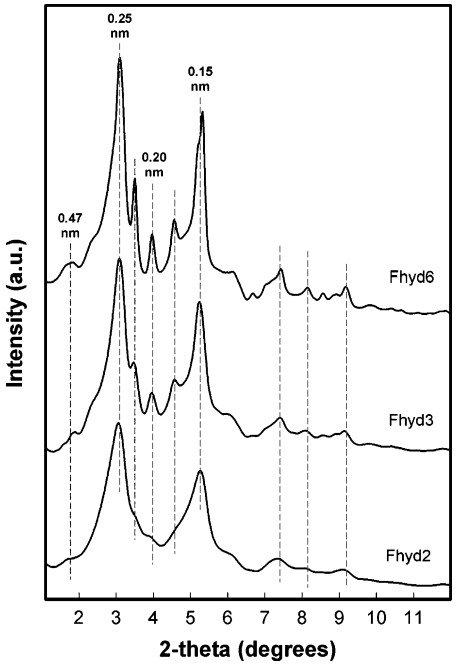

Figure 1. Background-subtracted diffraction data with intensity plotted in arbitrary units on the ordinate versus 2θ in degrees on the abscissa. The patterns from top to bottom are for 6, 3, and 2 nm ferrihydrite, respectively. The features in the pattern for Fhyd2 are relatively broadened and overlapping, although all of the diffraction maxima are the same, as indicated by the vertical dotted lines. The *d*-spacings for several of the commonly referenced maxima are indicated in nanometers.

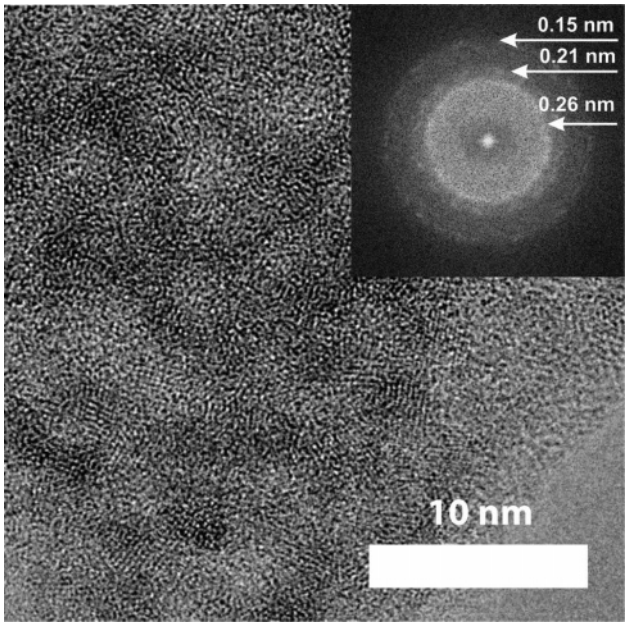

Figure 2. High-resolution transmission electron micrograph of Fhyd2. Individual particles appear to be on the order of 2−3 nm in diameter. Lattice fringes are present but difficult to discern because of a lack of contrast relative to support film on the TEM grid. The fast Fourier transform diffraction pattern taken from the whole area of the image is included as an inset. The calculated *d*-spacings for the most prominent diffraction rings are indicated.

High-Resolution Transmission Electron Microscopy (HRTEM). The results of HRTEM imaging for the three samples indicate that the average crystallite size ranges from 2 to 3 nm (Fhyd2) up to 5−7 nm (Fhyd6). The representative images (Figures 2−4) show that each sample consists of a relatively monodisperse population of nanocrystalline particles. Lattice fringes are subtle and not easily resolved (Figure 2) in part because these particles are extremely small and show similar contrast to the amorphous holey-carbon support film. The FFT diffraction pattern (Figure 2, inset) of the entire image shows distinct diffraction rings at 0.26, 0.21, and 0.15 nm. Figure 3 shows the representative image of sample Fhyd3, which was formed using the synthesis method for ∼4 nm nanoparticles. In contrast to Fhyd2, lattice fringes are more clearly visible, indicating a higher degree of crystallinity with most particles on the order of 3−4 nm

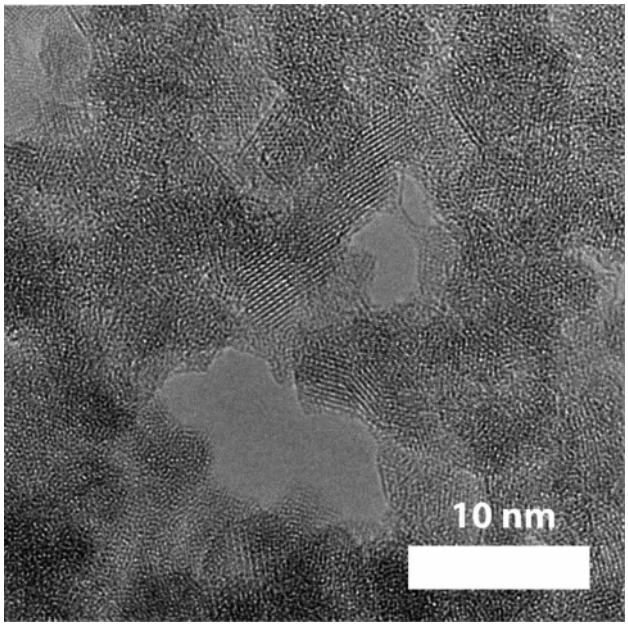

Figure 3. High-resolution transmission electron micrograph of Fhyd3. The particles appear to be on the order of 3−4 nm in diameter and show a higher degree of crystallinity than sample Fhyd2. The particles appear to be in preferred orientation on the TEM grid, suggesting a platelike morphology.

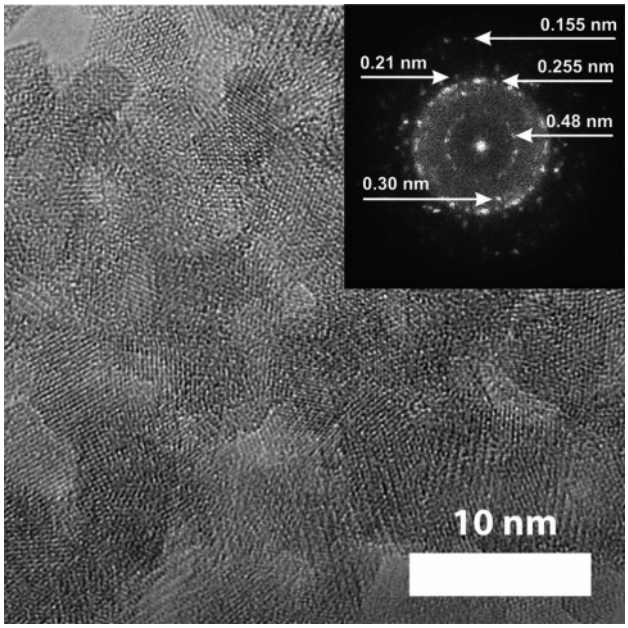

Figure 4. High-resolution transmission electron micrograph of Fhyd6. The particles show a higher degree of crystallinity than both Fhyd2 and Fhyd3, with average particle diameters of 5−7 nm. The particles also appear to be in preferred orientation on the TEM grid, suggesting a platelike morphology. The fast Fourier transform diffraction pattern taken from the whole area of the image is included as an inset. The calculated *d*-spacings for the most prominent diffraction spots are indicated.

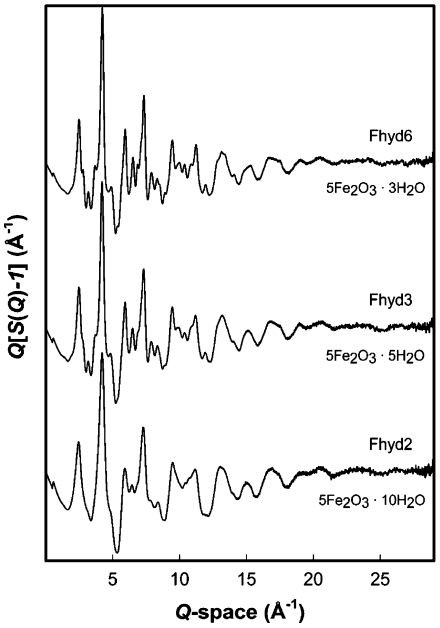

Figure 5. The weighted total scattering structure function $Q[S(Q)\text{-}1]$ properly normalized for ferrihydrite samples Fhyd2, Fhyd3, and Fhyd6 analyzed as dry powders. The three patterns show striking similarity in terms of the occurrences of diffraction maxima.

in diameter. Sample Fhyd6 (**Figure 4**) shows the highest degree of crystallinity, as evidenced by the particle sizes on the order of 5−7 nm and resolvable lattice fringes. The FFT diffraction pattern (Figure 4, inset) of the entire image shows strong diffraction features at 0.48, 0.30, 0.255, 0.21, and 0.155 nm. The measured *d*-spacings in the FFT patterns for Fhyd2 and Fhyd6 show good agreement with those observed in X-ray total scattering diffraction data (Figure 1). The full morphology of the nanoparticles is not easily discernible from HRTEM imaging alone but it appears that the particles are in preferred orientation on the TEM grids, suggesting they are platelike.

High-energy X-ray Total Scattering and Pair Distribution Function Analysis. The nominal formula for ferrihydrite ($5Fe_2O_3{\cdot}nH_2O$) was used during the normalization of the data to obtain $S(Q)$ and the resulting PDFs. To emphasize the diffuse components at high Q-values, we represented the data as $F(Q)$ or $Q[S(Q)\text{-}1]$ (Figure 5). The composition necessary for properly normalizing the data collected on powdered ferrihydrite precipitates was possible by adding small amounts of stoichiometric water (Figure 5, inset table) to the formula $5Fe_2O_3{\cdot}1H_2O$. Without this addition, the normalization of $S(Q)$ was only possible by subtracting additional background relative to the amount warranted on the basis of the equal exposure times used for both the sample and blank. The properly normalized patterns in Figure 5 again show obvious similarities in diffraction features even out in the region dominated by diffuse scattering between 15 and 30 $Å^{-1}$. The Fourier transform of $S(Q)$ ($\sim$30 $Å^{-1}$ for the dry samples in the present study) yields the PDF or $G(r)$, which is a real space representation of the atomic ordering of the material.[39] The resulting PDFs (Figure 6) confirm that

(39) Klug, H. P.; Alexander, L. E. *X-ray Diffraction Procedures for Polycrystalline and Amorphous Materials*, 2nd ed.; Wiley-Interscience: New York, 1974.

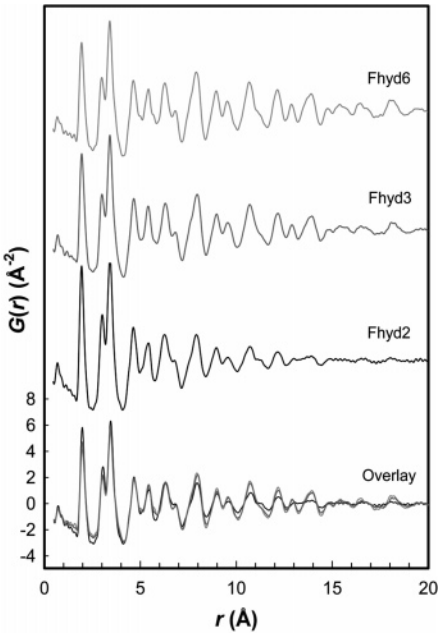

Figure 6. The PDF $G(r)$ vs distance r is plotted for Fhyd2, Fhyd3, and Fhyd6 analyzed as dry powders. The PDFs are nearly identical over 20 Å, indicating that these samples share the same structural arrangement. Beyond approximately 7 Å, the correlations for the 2 and 3 nm samples occur at the same distances but diminish more rapidly compared to those of the 6 nm sample. The bottom plot shows the overlay of the PDFs for the three samples.

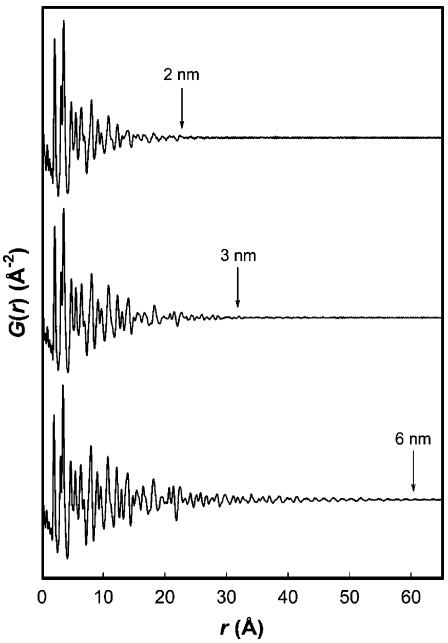

Figure 7. The PDF $G(r)$ plotted out to 65 Å to illustrate the degree of attenuation due to the range of structural coherence for Fhyd2 (top), Fhyd3, and Fhyd6 (bottom).

the short- and intermediate-range atomic ordering are nearly identical for the dry ferrihydrite precipitates examined. The PDFs for the same three precipitates analyzed in aqueous media (data not shown) are indistinguishable from those presented in Figure 6. As will be discussed, the PDF is not limited to the local ordering; it also provides atom pair correlations for all three samples beyond 15 Å and, in certain cases, can extend beyond 50 Å (Figure 7).

Thermogravimetric Analysis. TGA curves for Fhyd2, Fhyd3, and Fhyd6 show a relatively smooth weight loss,

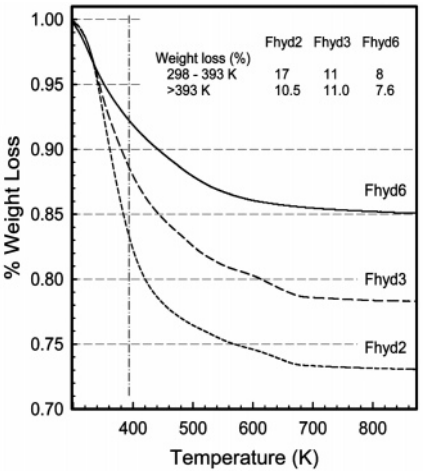

Figure 8. TGA results for samples Fhyd2, Fhyd3, and Fhyd6 showing percent weight loss as a function of temperature. The initial weight loss occurring between 298 and 393 K (see inset table) is primarily attributable to removal of surface-adsorbed water.

totaling 27.48, 21.96, and 15.57%, respectively (Figure 8). At temperatures ≤393 K, Fhyd2 lost ~17% by weight, or approximately 60% of its total weight loss. Fhyd3 and Fhyd6 lost ~11 and ~8% by weight, respectively, or approximately 50% of their total weight loss. The weight loss at lower temperatures (i.e., ≤393 K) is normally attributed to removal of surface-adsorbed water. On the basis of the TGA measurements, the stoichiometry for Fhyd2, Fhyd3, and Fhyd6 is $5Fe_2O_3 \cdot nH_2O$, with n equal to 10, 6, and 5, respectively. The TGA results presented here are generally consistent with previous studies.[15,40]

Discussion

The primary difference between the ferrihydrite precipitates formed by three different methods in this study is the size of the coherent scattering domains imposed by differences in average crystallite sizes. Until now, this idea has not been entirely appreciated since the time it was initially suggested by Drits et al. (1993).[20] The crystallinity of all the ferrihydrite precipitates examined in this study is relatively poor, in general, i.e., having broadened and weak XRD reflections (Figure 1). Also contributing to the broadening of maxima may be the effects of defects and disorder in the structure, which are manifested as a diffuse scattering component. These characteristics may have hindered prior structural studies of nanocrystalline ferrihydrite using crystallographic techniques, which rely on clearly defined Bragg peaks.

The PDFs for the precipitates show a significant degree of attenuation (Figure 7) due to limited coherent scattering domain sizes. The radial distance plotted along the abscissa is extended to 65 Å in Figure 7 to emphasize the difference in attenuation between the three samples. It is apparent that Fhyd2 exhibits the shortest range of structural coherence and therefore consists of the smallest average coherent scattering domain. The correlations in the PDF for Fhyd2 attenuate at a distance of approximately 20 Å and the remainder of the pattern (>20 Å) reduces to statistical noise. The correlations in the PDF for Fhyd3 attenuate slightly further out at approximately 3.0−3.2 nm and those of Fhyd6 show the greatest range of structural coherence extending out beyond 50 Å. These results clearly are consistent with the increased broadening of diffraction features illustrated in Figure 1 that occur with decreasing domain size. Direct imaging using HRTEM also indicates that Fhyd2, Fhyd3, and Fhyd6 differ in terms of average particle size and degree of crystallization (Figures 2 − 4). In the present study, as well as in other studies where ferrihydrite precipitates are imaged using HRTEM, the estimated average particle sizes reported are consistently slightly larger than what would be estimated on the basis of PDF analysis alone. The discrepancy may be in part attributable to variability in samples formed in different laboratories. However, in the present study, it is attributable to differences in what is fundamentally being measured by these techniques. In the case of HRTEM, the overall size of the visible particles are measured compared to PDF where the attenuation provides an indication of the average size of the coherent scattering domain. The PDF may not reflect atom pairs affected by surface relaxation and types of internal disorder that do not result in coherent scattering. In such cases, the estimated average size using PDF attenuation is always likely to underestimate the true size of a particle. These results are consistent with prior estimates in studies by other researchers using HRTEM[11,21] and those obtained in recent work on the same precipitates using STM and AFM.[12]

Table 2. Peak-Fitting of the PDF $G(r)$[a]

sample ID	first correlation r (Å)	second correlation r (Å)	third correlation r (Å)
Fhyd2	1.98(0)	3.03(7)	3.44(3)
Fhyd3	1.97(9)	3.03(4)	3.44(2)
Fhyd6	1.98(3)	3.03(1)	3.44(1)

[a] The positions from profile-fitting of the first three correlations in each PDF for the dry ferrihydrite precipitates.

An evaluation of the pair correlations between 1 and 20 Å in the PDFs for Fhyd2, Fhyd3, and Fhyd6 reveals that all share the same atomic arrangement (Figure 6**)**. The positions from profile fitting of the first three correlations are included in Table 2. The first correlation at ~2.0 Å suggests that Fe and O are predominantly in an octahedral coordination.[41] It has been suggested that tetrahedrally coordinated Fe−O may also be present in 2-line ferrihydrite[16] or possibly occur as the result of surface distortion resulting from the nanocrystalline particle sizes.[15,42] Evidence for this conjecture is not yet directly supported by PDF, but it should be noted that the difference in bond lengths in FeO_4 and FeO_6 polyhedra is only ~0.15 Å, for example, as is found in the structure of maghemite (γ-Fe_2O_3).[43] Additionally, distortions in the FeO_6 polyhedra would result in Fe−O bond lengths deviating from an ideal geometry and result in a broader correlation in the PDF at ~2.0 Å. Such a distortion would also have the

(40) Saleh, A. M.; Jones, A. A. *Clay Miner.* **1984**, *19* (5), 745−755.
(41) Shannon, R. D. *Acta Crystallogr., Sect. A* **1976**, *32* (SEP1), 751−767.
(42) Zhao, J.; Huggins, F. E.; Feng, Z.; Lu, F. L.; Shah, N.; Huffman, G. P. *J. Catal.* **1993**, *143* (2), 499−509.
(43) Greaves, C. *J. Solid State Chem.* **1983**, *49* (3), 325−333.

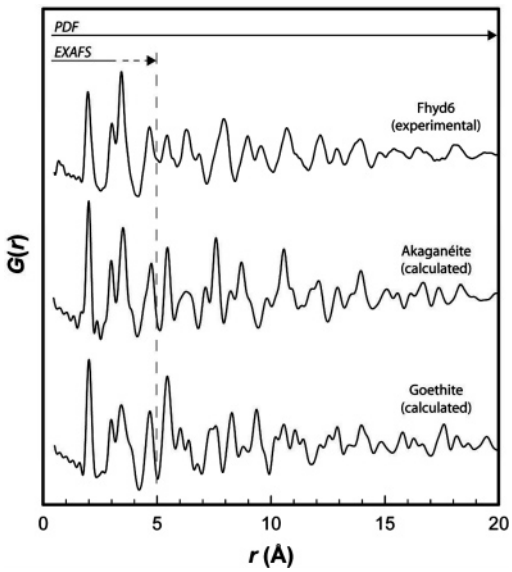

Figure 9. The experimental PDF $G(r)$ vs distance r is plotted for sample Fhyd6. Calculated PDFs for akaganéite and goethite are also plotted to show the similarities in the atom−atom distances over the first ~5 Å, typical of the range of distances reported by EXAFS. The PDF provides additional data that are essential for differentiating between competing structural models.

potential for obscuring the correlation corresponding to FeO_4 polyhedra, especially if the tetrahedrally coordinated Fe were in relatively minor abundance (i.e., <25%). In this circumstance, the contribution of FeO_4 to this region of the PDF would likely be manifested as a subtle asymmetry of the left side of the FeO_6 correlation. Such asymmetry is not obvious in the PDFs presented here but cannot be ruled out for the reasons described above. The second and third correlations at 3.03 and 3.44 Å are characteristic of Fe−Fe distances for FeO_6 polyhedra linked in edge-sharing and corner-sharing configurations, respectively. These distances and configurations are consistent with prior EXAFS work on ferrihydrite[44] and do not suggest the presence of polyhedra in the face-sharing configuration that has been suggested in prior work.[16,17,19]

The main advantage to using high-energy X-ray scattering and PDF analysis over spectroscopic techniques such as EXAFS for comparing ferrihydrite with different particle sizes, and ultimately comparing its structure, is that the PDF is not limited to information associated with the first three shells. As one recent study of nanocrystalline MnS demonstrated, multiple structural models may provide a satisfactory fit when considering only the short-range atomic order (approximately <5 Å).[35] In the Fe−O−H system, there are a number of potential structural models that have edge- and corner-sharing octahedra and thereby result in a very similar radial distribution function to ferrihydrite (e.g., goethite, akaganéite) out to ~5 Å (Figure 9). The PDF provides the invaluable additional information on the intermediate-range atomic order that we predict, in the case of ferrihydrite, will eventually allow for the differentiation between competing models.

(44) Combes, J. M.; Manceau, A.; Calas, G. *Geochim. Cosmochim. Acta* **1990**, *54* (4), 1083−1091.

Variability in the quality of samples formed in separate laboratories using different starting materials and with subtle variations in synthesis conditions has been identified as a possible source of complexity and reason for disagreement between previous studies of structure and composition.[4] Our study also included PDF analysis of three samples made by independent groups at BNL, Temple, and Stony Brook University, with all using the same general preparation method.[13] The PDFs for the three samples (not shown) were virtually identical, suggesting no significant differences in structure or domain size. The potential structural changes in ferrihydrite caused by the interaction of the nanocrystalline solid phase with aqueous solution were evaluated by also analyzing the precipitates (Fhyd2, Fhyd3, and Fhyd6) redispersed in aqueous solution. Again, no discernible changes for ferrihydrite nanoparticles in either state were observed in the resulting PDFs (also not shown). Although stoichiometric water was added as part of the normalization in both wet and dry samples, the abundance of structural water is still uncertain. Prior work has suggested that the presence of hydroxyl is essential for maintaining the ferrihydrite structure,[45] although this idea has also been disputed.[9,10,14] On the basis of the formula used to normalize the data in the present study, it is necessary to have only 1 water (2 protons) in the structure to charge-balance the Fe and O. TGA curves show a significant weight loss for each sample at temperatures ≤393 K (Figure 8), indicating the removal of weakly bound surface-adsorbed water. This evidence for the presence of variable amounts of surficial water provides support for the additional H_2O necessary during the PDF normalization procedure and is in good agreement with the stoichiometry estimated from TGA. Subsequent weight loss at temperatures >393 K may indicate the loss of more strongly bound structural water and is not yet fully understood. We currently have experiments in progress using neutron scattering and PDF analysis on samples of ferrihydrite synthesized carefully with deuterium to minimize the incoherent scattering interference resulting from hydrogen contamination. This study will be essential for understanding the role of protons in the structure of ferrihydrite and will be a part of future communications.

Conclusions

With the development and application of advanced analytical and experimental techniques at synchrotron facilities and in the laboratory, we now have the tools to rigorously characterize fundamental atomic properties of traditionally challenging materials, such as nanocrystalline ferrihydrite. On the basis of PDF analysis of high-energy X-ray total scattering data, the primary difference between so-called 2- and 6-line ferrihydrite is the limited size of the coherent scattering domains imposed by differences in average primary crystallite size, rather than a fundamental difference in atomic arrangement. A comparison of the PDFs for the samples with three distinct average particle sizes in this study indicates that all share the same atomic arrangement on the basis of the atom pair correlations extending beyond 15 Å.

(45) Childs, C. W.; Kanasaki, N.; Yoshinaga, N. *Clay Sci.* **1993**, *9* (2), 65.

The average domain sizes of the precipitates examined in this study are estimated using the PDF method to be in the range of 2−6 nm and are supported by HRTEM. The local atomic arrangement from PDF analysis also does not show any significant changes when analyzed in powder form or when redispersed in aqueous media. Surface-adsorbed water content varied with particle size, as indicated by both PDF analysis and TGA. The results presented here provide the foundation for quantitatively testing previously proposed structural models for ferrihydrite and may lead to the development of a new structural model that better describes this phase. These ideas will be explored in future communications.

Acknowledgment. This study is supported by the Center for Environmental Molecular Science (CEMS) and the National Science Foundation (NSF) (Awards CHE0221934, DMR-045244, and EAR-0510501) and the U.S. Department of Education through the GAANN Program Sponsor ID: P200A060248. High-energy XRD measurements were performed at X-ray Operation and Research (XOR) beamlines 1-ID-C and 11-ID-B at the Advanced Photon Source, Argonne National Laboratory. Use of the APS is supported by the U.S. Department of Energy (DOE), Office of Science, Office of Basic Energy Sciences, under Contract DE-AC02-06CH11357. Use of the HRTEM is supported by the U.S. DOE under Contract DE-AC02-98CH10886.

Supporting Information Available: $G(r)$ versus r plots for 2 nm ferrihydrite formed in different laboratories. This material is available free of charge via the internet at http://pubs.acs.org.

CM062585N